

ChemComm

Accepted Manuscript



This is an *Accepted Manuscript*, which has been through the Royal Society of Chemistry peer review process and has been accepted for publication.

Accepted Manuscripts are published online shortly after acceptance, before technical editing, formatting and proof reading. Using this free service, authors can make their results available to the community, in citable form, before we publish the edited article. We will replace this *Accepted Manuscript* with the edited and formatted *Advance Article* as soon as it is available.

You can find more information about *Accepted Manuscripts* in the [Information for Authors](#).

Please note that technical editing may introduce minor changes to the text and/or graphics, which may alter content. The journal's standard [Terms & Conditions](#) and the [Ethical guidelines](#) still apply. In no event shall the Royal Society of Chemistry be held responsible for any errors or omissions in this *Accepted Manuscript* or any consequences arising from the use of any information it contains.

COMMUNICATION

3D graphene network@WO₃ nanowires composite: a multifunctional colorimetric and electrochemical biosensing platform

Cite this: DOI: 10.1039/x0xx00000x

Received 00th January 2012,
Accepted 00th January 2012Ye Ma,^a Minggang Zhao,^a Bin Cai,^a Wei Wang,^a Zhizhen Ye,^{ab} Jingyun Huang,^{*ab}

DOI: 10.1039/x0xx00000x

www.rsc.org/

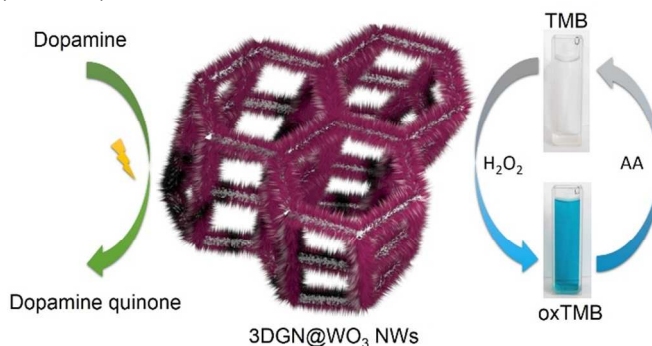
A three dimensional graphene network (3DGN)@WO₃ nanowires (NWs) sensor is proposed which can perform colorimetric and electrochemical sensing techniques to detect H₂O₂, ascorbic acid and dopamine. The 3DGN provides three functions: anchoring, separating, conducting, while the WO₃ NWs maximize surface area and catalyze reactions.

Natural enzymes, though possess high specificity and high catalytic activity are usually vulnerable to dramatic changes of environment. This drawback induces intense researches on enzyme mimics which is low-cost, simple to synthesize and much more stable under harsh environments. It has been found that numerous nanomaterials possess intrinsic capability to catalyze the oxidation and reduction of H₂O₂ as peroxidase mimics.¹⁻³ As most researches indicated the smaller the particles are, the more efficient the peroxidase mimics would be.⁴ But the downscaling of particle size would also result in some problems. To most nanomaterials, the recycle of the peroxidase mimics is always a challenge, for once dispersed into the solution, they are impossible to separate unless employing vigorous centrifuge.⁵ With regard to magnetic nanoparticles, they could be easily recollected from the solution by magnets. But the magnetized particles when dispersed into the solution are more likely to aggregate which as a result deteriorates their catalytic efficiency.^{4,6} To simplify the separation procedure and maximize the peroxidase-like activity, a structure of 3D network with high catalytic nanomaterials embedded would be favourable.

In most practical detections or diagnoses, a fast and cheap qualitative test is often preferable before a more elaborate and quantitative test.⁷ Transforming the detection events into colour changes, colorimetric biosensing are fast responding, low-cost and readable to naked eyes. These advantages gain colorimetric sensors great popularity in qualitative self-help tests. However, the sensitivity and linearity of colorimetric sensors are still not competitive to electrochemical sensors which though, are often delicate, requiring the connection to signal analysis instruments.⁸ Until now, there is still no single device can combine the advantages of colorimetric and electrochemical sensors and integrate both techniques in one device.

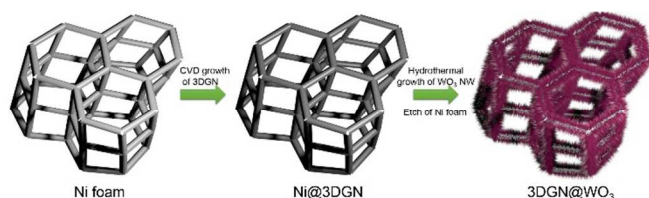
Therefore, our aim is to synthesize a sensing platform which not only possesses a freestanding 3D structure, peroxidase-like activity and high electrochemical sensitivity, but also integrates the

two orthogonal sensing methods: colorimetric and electrochemistry (Scheme 1).



Scheme 1 Schematic representation of 3DGN@WO₃ colorimetrically detecting H₂O₂ and AA and electrochemically detecting dopamine.

As one of the most promising materials, graphene, though has good mechanical strength and outstanding electrical properties, is always two-dimensional sheet whose morphology cannot be easily changed which limits its active surface area and further applications.⁹ Very recently, there emerged a new form of graphene: three-dimensional graphene networks (3DGN), a seamlessly connected porous carbon network¹⁰ whose unique 3D macroporous structure could be an ideal conductive and supportive freestanding scaffold to accommodate catalyst, collect electrical signals, buffer analytes and ease the separation process in colorimetric or electrochemical detections. Among various metal oxides, WO₃ has many advantages such as simple synthesis, high catalytic activity, good chemical stability and strong adherence to substrates.¹¹ However, WO₃ is rarely used in colorimetric or electrochemical biosensors. With the CVD growth of 3DGN and hydrothermal growth of WO₃ nanowires (NWs Scheme 2), we combined the merits of 3DGN and WO₃ to obtain a multifunctional sensing platform that integrate colorimetric and electrochemical methods to detect H₂O₂, AA and dopamine.



Scheme 2 Synthesis process of 3DGN@WO₃ NWs array.

The digital image in Fig. 1a shows the macroscale 3DGN@WO₃ (left) and 3DGN (right). It could be seen that 3DGN have good mechanical strength that the whole structure is self-supporting, while comparing with 3DGN, the 3DGN@WO₃ on the right is tinted yellow which indicates that WO₃ NWs are evenly anchored on 3DGN. The weight of 1.5 mm × 1 cm × 1 cm 3DGN and 3DGN@WO₃ is about 0.8 mg and 5.3 mg respectively. The low to high magnification SEM images of 3DGN@WO₃ are shown in Fig. 1b-d. A three dimensionally interconnected network with pores from 100 μm to 300 μm in diameter can be clearly observed in Fig. 1b. With no crack or breaks, the hollow graphene bridge is about 50 μm wide where WO₃ NWs are uniformly located. Fig. 1d features the structure of WO₃ NWs array whose diameter is about 20 nm. The 3DGN offers a favourable structure to immobilize bioactive molecules, to facilitate mass transfer and to collect the signals of reactions, while the WO₃ NWs array provide large active surface area to catalyse reactions.

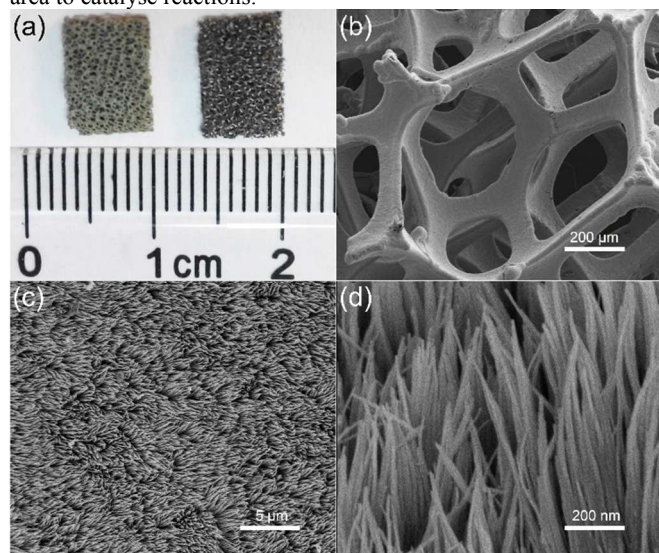


Fig. 1 Morphology of 3DGN@WO₃. (a) Digital image of 3DGN@WO₃ (left) and 3DGN (right); (b-d) Low to high magnification SEM images of 3DGN@WO₃.

The composition of 3DGN@WO₃ were first examined by XRD (Fig. S2) in which all the peaks can be attributed to either 3DGN or WO₃. In the Raman spectra of 3DGN (Fig. S3), two characteristic peaks, G and 2D peaks at 1581 cm⁻¹ and 2725 cm⁻¹ respectively can be easily observed and no peaks at 1350 cm⁻¹ indicates good quality and the lack of defects.¹² As XPS analysis shows, the three characteristic peak of WO₃, namely W4f_{7/2} at 35.7 eV, W4f_{5/2} at 37.8 eV and W5p_{3/2} at 41.7 eV confirm the successful growth of WO₃ NWs array on the 3DGN (Fig. S4).¹³ The Nyquist plots of electrochemical impedance spectroscopy (Fig. S5) shows that the impedance of 3DGN@WO₃ (43.52 Ω) is relatively smaller than that of bare 3DGN (52.66 Ω) and WO₃/GCE (144.7 Ω) due to the large active surface area and high electrochemical activity of WO₃ NWs array on the highly conductive 3DGN.

To investigate the peroxidase-like activity of 3DGN@WO₃ and to colorimetrically detect H₂O₂, 3, 3', 5, 5'-tetramethylbenzidine (TMB) was used as the chromogenic substrate, which in the present of H₂O₂ would be catalysed by 3DGN@WO₃ from colourless to sky blue (maximum absorbance 652 nm).

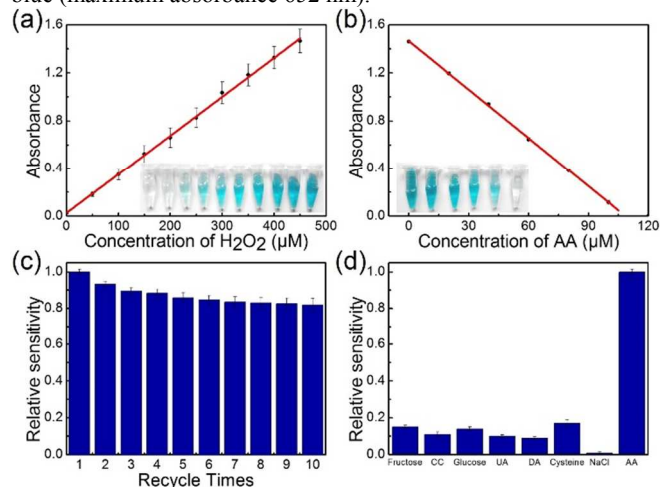
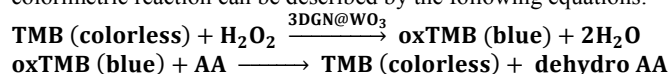


Fig. 2 Colorimetric sensing of H₂O₂ and AA in 0.5 mM TMB 0.1 M PBS solution. (a-b) The calibration curve of absorbance at 652 nm versus the concentration of H₂O₂ and AA; (c) Recycling property of 3DGN@WO₃; (d) Selectivity of 3DGN@WO₃ to AA with adding 40 μM fructose, choline chloride (CC), glucose, uric acid (UA), dopamine (DA), cysteine (CS) and NaCl respectively.

First, we compared the catalytic activity of 3DGN@WO₃, 3DGN and WO₃ powder in 0.5 mM TMB 0.4 mM H₂O₂ 0.1 M PBS solution (Fig. S6). Though the peroxide-like activity of these samples are time dependent, it could be clearly observed that the efficiency of 3DGN@WO₃ is much better than that of bare 3DGN which highlight the vital role of WO₃ NWs. And due to the aggregation of WO₃ NWs, the WO₃ powder alone shows inferior peroxidase-like activity than 3DGN@WO₃. To quantify the colour change of TMB from colourless to blue, the calibration curve of the absorbance to the concentration of H₂O₂ is plotted in Fig. 2a: Abs = 0.02604 + 0.00325 [H₂O₂] (R = 0.999) demonstrating a good linearity (up to 450 μM) and high sensitivity of 3DGN@WO₃ NWs which ensure the accuracy of H₂O₂ detection.

Then the capability of 3DGN@WO₃ to detect ascorbic acid (AA) is investigated. After adding 450 mM H₂O₂ to trigger the blue colour change in 5 min, 0-100 mM AA is added into the solution and induces rapid fading of the blue colour of oxTMB (Fig. 2b). The resultant correction equation of absorbance to the concentration of AA is Abs = 1.465 - 0.01349 [AA] (R = 0.999). Moreover, the proportional relationship between the concentration of AA and the decay of absorbance peak is very steady: even after ten times recycling, the sensitivity is still above 80% (Fig. 2c). In order to test the selectivity of the catalytic reduction of oxTMB, the influence of some other possible coexisting substances in human blood serum is examined (Fig. 2d). There are no apparent changes of absorbance with the addition of 40 μM fructose, choline chloride (CC), glucose, uric acid (UA), dopamine (DA), cysteine (CS) and NaCl respectively, indicating a good specificity to AA.

As we know, H₂O₂ is an active oxidizing agent but cannot oxidize TMB directly without the aid of catalyst, while AA is a naturally occurring organic compound with antioxidant properties. The whole colorimetric reaction can be described by the following equations:



For the first part, it is a typical Fenton-type reaction as many other peroxidase mimics.^{14, 15} The WO_3 induced oxidizing radical $\bullet\text{HO}$ from H_2O_2 is a reactive oxidant which oxidizes the colourless TMB into blue oxTMB.^{16, 17} When AA is added, the two-electron reduction of oxTMB to TMB occurs and the colour changes from blue to colourless.

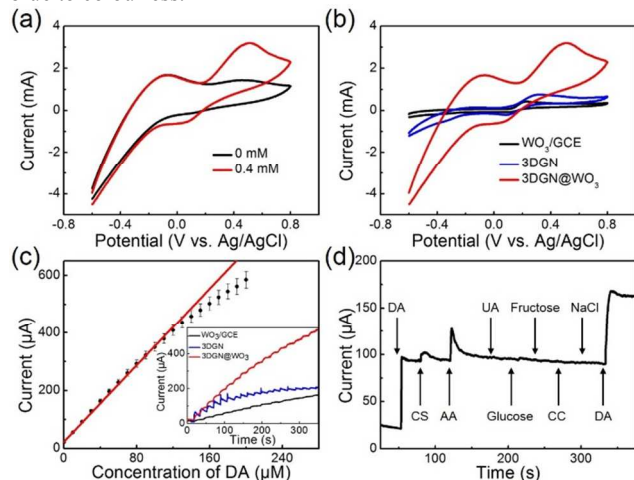


Fig. 3 Electrochemical sensing of dopamine. (a) CV curves of 3DGN@ WO_3 in 0 and 0.4 mM dopamine solution at the scan rate of 50 mV/s; (b) CV curves of WO_3 , 3DGN and 3DGN@ WO_3 in 0.4 mM dopamine solution; (c) Dose response curve of 3DGN@ WO_3 composite at the potential of 0.3 V, with a linear fitting at lower concentration range. The inset shows the amperometric responses toward successive addition of 10 μM dopamine per time; (d) Amperometric i-t response to the addition of 20 μM DA, CS, AA, UA, glucose, fructose, CC, NaCl and DA.

Dopamine is a hormone and neurotransmitter that plays a number of important roles in the human brain and body.¹⁸ To investigate the electrochemical sensing property of 3DGN@ WO_3 to dopamine, firstly cyclic voltammetry (CV) is employed to show the different responses with and without dopamine (Fig. 3a). Clearly, an oxidation peak at about 0.49 V appears when 0.4 mM dopamine is added into the solution. When increase the scan rate from 50 to 100 mV/s, both the potential and current of the oxidation increase (Fig. S7) indicating a mass transfer controlled process.¹⁹ The different responses of WO_3 NWs, 3DGN and 3DGN@ WO_3 to dopamine is manifested in Fig. 3b, where the CV curve of 3DGN@ WO_3 is dramatically enhanced comparing with that of bare 3DGN and WO_3 NWs only, suggesting impressive signal collecting function of 3DGN and the high electrocatalytic activity of WO_3 NWs array. On the grounds that the oxidation reaction of dopamine is controlled by diffusion, the Randles-Sevcik equation²⁰ then can be utilized to compare the electrochemical active surface area (ECSA) of WO_3/GCE , 3DGN and 3DGN@ WO_3 . According to the equation, ECSA is proportional to the peak current of both sensors, therefore the ECSA of 3DGN@ WO_3 is four times to that of 3DGN (3.199 mA to 0.7595 mA) and seven times to that of WO_3/GCE (0.4210 mA), suggesting the key role of WO_3 NWs in enlarging the surface area on 3DGN and the indispensable function of 3DGN in conducting and anchoring WO_3 .

Holding at the potential of 0.3 V in 0.1 M PBS (pH 7.2) the calibration curve of current versus dopamine concentration is plotted in Fig. 3c. An ultrahigh sensitivity of 1.306 $\text{mA mM}^{-1} \text{cm}^{-2}$ (R.S.D. of three samples is 4.56%) is obtained and the resultant linear range is up to 150 μM ($R = 0.997$), lowest detection limit 238 nM ($S/N = 3$) and the response time 4 s. The comparison of amperometric i-t responses of WO_3/GCE , 3DGN and 3DGN@ WO_3 is plotted in Fig. 3c inset. Although the WO_3/GCE have a long linear range and the bare 3DGN have the noticeable sensitivity at the low concentration

region, WO_3 NWs alone suffer low sensitivity and the performance of 3DGN deteriorates fast with the successive addition of dopamine. By contrast, the sensitivity of 3DGN@ WO_3 almost triples that of WO_3 alone and can remain at a relatively long range of concentration which demonstrates its good stability (also see Fig. S8) and fast desorbing speed of redox product. At last, the selectivity of 3DGN@ WO_3 is manifested in Fig. 3d. Obviously, the sensor presents good specificity to dopamine and can eliminate the interference of fructose, glucose, UA, AA, CC, CS and NaCl.

The macroporous network of 3DGN play a key role in buffering electrolytes to minimize the diffusion distance to the surface of WO_3 NWs which results in fast sensing response. Thanks to its superior conductivity, the 3DGN can collect signals from vast range of reaction sites and transmit them rapidly to the analyser. At the same time, on the surface of WO_3 occurs the redox of dopamine: $\text{WO}_3 + x\text{H}^+ + \text{DA} \rightarrow \text{H}_x\text{WO}_3 + \text{DA quinone}$.²¹ WO_3 NWs array can further boost the response of dopamine due to its large nanoscale surface area and electrocatalytic properties. Therefore, it is the synergetic combination of 3DGN and WO_3 NWs that induce the outstanding sensing property.

To summarize, a facile synthesis route of 3DGN@ WO_3 nanowires array using CVD and hydrothermal method was prompted. For the first time, this sensor is demonstrated to have the intrinsic peroxidase-like activity to colorimetrically detect H_2O_2 and AA and electrochemically detect dopamine. The 3DGN possesses outstanding mechanical strength and light weight to serve as a monolithic freestanding sensing scaffold. In the colorimetric detection, thanks to its macroscale network with large surface area, 3DGN can uniformly accommodate nanoscale catalyst without aggregation and make the separation of the catalyst from solution much easier than traditional catalytic particles which are vulnerable to aggregation and difficult to separate. In electrochemical detection, the foam like structure of 3DGN acts as an electrolytes reservoir to shorten the diffusion distance and as a current collector to boost electrical sensitivity. Meanwhile, as the main catalyst in both colorimetric and electrochemical sensing, the WO_3 NWs maximize the reactive surface area, show high peroxidase-like and electrocatalytic activities. Considering that its unique hierarchical 3D structure is beneficial to mimic 3D environment of cell living, 3DGN@ WO_3 has the potential to function both as scaffold supporting cells and as a real-time sensor monitoring analytes mimicking in vivo condition.

This work was financially supported by National Natural Science Foundation of China (9133203), Natural Science Foundation of Zhejiang province (LY14E020006) and the Doctorate Fund of the Ministry of Education under grant no. 2011010110013.

Notes and references

^a State Key Laboratory of Silicon Materials, Department of Materials Science and Engineering, Zhejiang University, Hangzhou 310027, China. E-mail: huangjy@zju.edu.cn

^b Cyrus Tang Center for Sensor Materials and Applications, Zhejiang University, Hangzhou 310058, China

† Electronic Supplementary Information (ESI) available:

1 W. W. He, X. C. Wu, J. B. Liu, X. N. Hu, K. Zhang, S. A. Hou, W. Y. Zhou and S. S. Xie, *Chem. Mater.*, 2010, **22**, 2988-2994.

2 Y. J. Song, W. L. Wei and X. G. Qu, *Adv. Mater.*, 2011, **23**, 4215-4236.

3 J. Xie, X. Zhang, H. Wang, H. Zheng, Y. Huang, *Trac-Trends Anal. Chem.*, 2012, **39**, 114-129.

4 L. Gao, J. Zhuang, L. Nie, J. Zhang, Y. Zhang, N. Gu, T. Wang, J. Feng, D. Yang, S. Perrett and X. Yan, *Nat. Nanotechnol.*, 2007, **2**, 577-583.

5 M. Liu, H. Zhao, S. Chen, H. Yu and X. Quan, *ACS Nano*, 2012, **6**, 3142-3151.

6 Y. Fan and Y. Huang, *Analyst*, 2012, **137**, 1225-1231.

7 B. Etemad and D. C. Whitcomb, *Gastroenterology*, 2001, **120**, 682-707.

8 A. Chaubey and B. D. Malhotra, *Biosens. Bioelectron.*, 2002, **17**, 441-456.

- 9 X. Huang, Z. Yin, S. Wu, X. Qi, Q. He, Q. Zhang, Q. Yan, F. Boey and H. Zhang, *Small*, 2011, **7**, 1876-1902.
- 10 Z. Chen, W. Ren, L. Gao, B. Liu, S. Pei and H. Cheng, *Nat. Mater.*, 2011, **10**, 424-428.
- 11 S. K. Deb, *Sol. Energy Mater. Sol. Cells*, 2008, **92**, 245-258.
- 12 A. C. Ferrari, J. C. Meyer, V. Scardaci, C. Casiraghi, M. Lazzeri, F. Mauri, S. Piscanec, D. Jiang, K. S. Novoselov, S. Roth and A. K. Geim, *Phys. Rev. Lett.*, 2006, **97**, 4.
- 13 A. P. Shpak, A. M. Korduban, M. M. Medvedskij and V. O. Kandyba, *J. Electron Spectrosc. Relat. Phenom.*, 2007, **156**, 172-175.
- 14 W. B. Shi, X. D. Zhang, S. H. He and Y. M. Huang, *Chem. Commun.*, 2011, **47**, 10785-10787.
- 15 J. Xie, H. Cao, H. Jiang, Y. Chen, W. Shi, H. Zheng and Y. Huang, *Anal. Chim. Acta*, 2013, **796**, 92-100.
- 16 J. L. Dong, L. N. Song, J. J. Yin, W. W. He, Y. H. Wu, N. Gu and Y. Zhang, *ACS Appl. Mater. Interfaces*, 2014, **6**, 1959-1970.
- 17 X. H. Wang, K. G. Qu, B. L. Xu, J. S. Ren and X. G. Qu, *Nano Res.*, 2011, **4**, 908-920.
- 18 K. C. Berridge and T. E. Robinson, *Brain Res. Rev.*, 1998, **28**, 309-369.
- 19 Y. Ma, M. Zhao, B. Cai, W. Wang, Z. Ye and J. Huang, *Biosens. Bioelectron.*, 2014, **59**, 384-388.
- 20 M. n. G. Martin, M. L. Rodríguez-Méndez and J. A. de Saja, *Langmuir*, 2010, **26**, 19217-19224.
- 21 Q. Mi, R. H. Coridan, B. S. Brunshwig, H. B. Gray and N. S. Lewis, *Energy Environ. Sci.*, 2013, **6**, 2646-2653.